LWT - Food Science and Technology 169 (2022) 114062

Contents lists available at ScienceDirect

LWT

journal homepage: www.elsevier.com/locate/lwt

Comparison and prediction of UV-C inactivation kinetics of *S. cerevisiae* in model wine systems dependent on flow type and absorbance

Benedikt Hirt [a,*], Jaayke Fiege [a], Svetlana Cvetkova [b], Volker Gräf [a], Maren Scharfenberger-Schmeer [b], Dominik Durner [b], Mario Stahl [a]

[a] Department of Food Technology and Bioprocess Engineering, Max Rubner-Institut, Federal Research Institute of Nutrition and Food, Haid-und-Neu-Straße 9, 76131, Karlsruhe, Germany

[b] Institute for Viticulture and Enology, Dienstleistungszentrum Laendlicher Raum (DLR) Rheinpfalz, Breitenweg 71, 67435, Neustadt an der Weinstrasse, Germany

ARTICLE INFO

Keywords:
UV-C inactivation
UV-C reactor
Saccharomyces cerevisiae D576
Weibull model
Iodide/iodate actinometry

ABSTRACT

UV-C (254 nm) treatment can be an alternative or supplement method to adding sulfite to wine for stabilization. There are various types of UV-C reactors using different flow types. However, literature data often refer to specific microorganisms in specific food using specific UV-C reactors. Therefore, a statement about the influence of the flow conditions on the inactivation of microorganisms is difficult. This study examined the inactivation of *Saccharomyces cerevisiae* dependent on the flow conditions. Different flow conditions were realized in three UV-C reactor types. In order to minimize the influence of the natural fluctuations of the ingredients in wine, a model medium was introduced and validated to mimic the inactivation of *S. cerevisiae* in wine. The absorbance of the model solution was adjusted to resemble wine available on the market by applying variable concentration of food coloring (sunset yellow). These model solutions with inoculated microorganisms were UV-C treated using different flow conditions (Dean vortices, turbulent and laminar tube flows, and laminar annular thin film flows with a 3 mm and a 0.6 mm gap). Mathematical models were established to predict the inactivation of *S. cerevisiae* dependent on the flow type, the absorbance of the (model) wine and the UV-C dose.

1. Introduction

Microorganisms in winemaking are used to convert sugar into alcohol, reduce wine acidity and introduce desirable flavors to the wine. Conversely, they can cause numerous unwelcome wine spoilage problems, which reduce wine quality and value. The strongest selection pressure against yeast and bacteria in wine is high ethanol content, acidity and limited amount of nutrients. Nevertheless, there are still organisms that can live in some wines and spoil them by causing off-flavors. The common way to stabilize wine is the addition of sulfites. However, the acceptance by the consumer for sulfites in wine and additives in general is decreasing (Costanigro et al., 2014; Vecchio et al., 2021). There is a demand for alternative methods for stabilization. This study examined the application of UV-C energy as an alternative or supplementary process. UV-C treatment alone cannot substitute sulfites fully, since the secondary task of sulfites is serving as antioxidant. Other alternatives for example are flash pasteurization, high pressure (Buzrul, 2012), high power ultra sound (Morata et al., 2012) and pulsed electric field treatments (PEF) (Puértolas et al., 2010).

There are many studies concerning the UV-C treatment of liquid food. Some studies like Ngadi et al. (2003) and Unluturk et al. (2010) investigated the inactivation of organisms in a collimated beam apparatus. Others like Xiang et al. (2020) and Baykuş et al. (2021) treated liquid food in petri dishes underneath UV sources. A majority of studies are more application oriented and investigated the inactivation in flow through UV-C reactor systems. The main challenge regarding an efficient UV-C treatment of liquid food is the low penetration depth of UV-C radiation into opaque liquids. The penetration depth d in a solution can be determined with the Lambert-Beer law:

$$I(d) = I_0\ 10^{\varepsilon_\lambda \cdot c \cdot d_p} \tag{1}$$

Where $I(d)$ is the UV-C Irradiance at a given penetration depth, I_0 is the irradiance at $d = 0$, ε_λ is the extinction coefficient and c the concentration of the absorbent substance. Therefore, the design of the reactor is crucial for a homogenous dose distribution in the entire liquid. There are several types of UV-C reactors using different flow patterns. In

* Corresponding author.
E-mail address: Benedikt.Hirt@mri.bund.de (B. Hirt).

https://doi.org/10.1016/j.lwt.2022.114062
Received 17 May 2022; Received in revised form 5 September 2022; Accepted 3 October 2022
Available online 4 October 2022
0023-6438/© 2022 The Authors. Published by Elsevier Ltd. This is an open access article under the CC BY license (http://creativecommons.org/licenses/by/4.0/).

general, four flow types can be found in studies and publications: Laminar and turbulent flow, Dean-Vortex and Taylor-Couette flow. In order to achieve these flow conditions, different reactor designs or systems are usually used. One used reactor type is the coiled tube Dean-Vortex reactor (Barut Gök, 2021; Fenoglio et al., 2020; Müller et al., 2014). Some researchers like Junqua et al. (2020) use a coiled tube reactor for turbulent flow with Reynolds numbers up to 19,000. There are already commercially available reactors from manufacturers like UVivatec® Lyras® or Trojan Technologies®. Another reactor design uses an annular thin film or concentric pipe. These reactors are used with laminar (Koutchma, 2008) and turbulent flow (Crook et al., 2015; Pendyala et al., 2021) The reactor type is also commercially available with turbulent flow in a concentric pipe: Surepure® and Cidersure®. Both reactors have an FDA approval for the UV-C treatment of apple cider. The UV-C treatment in a Taylor Couette flow is examined e.g. from Giorges et al. (2008). A commercial application in the food sector is not known to the authors.

In most of these studies UV-C systems were investigated using specific liquid food with specific organisms. This results in different flow types, Reynolds numbers etc. for each study. Therefore, a comparison of the different systems is difficult or impossible. Furthermore, different methods were used to determine the applicated UV-C dose, that makes a comparison even more difficult. The most used applied method to determine the UV-C dose is the iodide/iodate actinometry according to R. O. Rahn (1997), biodosimetry to determine the UV-C energy that reaches the organisms and calculation via the emitted UV-C power with regard to the dwell time behavior. Koutchma and Parisi (2004) used *E. coli* K12 as a biodosimeter to determine the dose distribution of the UV-C reactors. The biodosimetry disregards the UV-C dose that is absorbed by the wine ingredients. This absorbed UV-C light can entail a change in flavor and color of a wine if the dose exceeds a wine specific level (Golombek et al., 2021). Therefore, the total UV-C dose that is absorbed by the liquid and the organisms is regarded in this study.

Different prototype UV-C reactors have been developed and constructed to compare the inactivation of *Saccharomyces cerevisiae* as a model organism for different flow pattern in different absorbing fluids. The optical density of a model solution was varied resulting in different inactivation kinetics. The model solutions were validated by adjusting the absorbance (7-50), pH-value (2.5–7), and ethanol content (0–15%) and comparing the inactivation kinetics to the ones in wine.

2. Materials and methods

Unless otherwise described, all chemicals were purchased from Sigma-Aldrich. The absorbance/optical density was measured with a Unicam UV-VIS Spectrometer. The turbidity measured in nephelometric turbity units (NTU) was quantified with a Turbiquant® 3000 IR. The pH-value was determined with a WTW inoLab pH 720. The dynamic viscosity was measured with a rheometer (Thermo Scientific Haake MARS 60). The density was studied with a flexural resonator (Heraeus/Paar DMA 60). All measurements were taken in triplets and the means were determined with their respective deviation.

2.1. Properties of the applied wines

Four different wines were used in this study to compare the UV-C inactivation of *Saccharomyces cerevisiae* to the inactivation in its respective model solutions. The wines were provided by DLR Weincampus in Neustadt, Germany, and are from 2019.

2.2. UV reactors

Koutchma et al. (2016) stated that in order to describe an UV-C reactor or UV-C treatment system, the lamp characteristics, the number of lamps and their power, lamp wavelength, the flow conditions and the number of passes through the reactor should be described. Also the UV-C irradiance distribution and the residence time distribution are needed to evaluate the performance of UV-C reactors (Atilgan et al., 2021). The following three different types of UV- C reactors were used for this study.

2.2.1. Annular thin film reactor TFR

The reactor (Fig. 1) has a 20 W low-pressure mercury (LPM) lamp (UVPro FMD Series) as a UV-C source with 7.5 W emitted UV-C power at its wavelength peak of 253.6 nm. The lamp is surrounded by a quartz tube with an outer diameter of approx. 23.10 mm. The reactor has an inner diameter of approximately 29.24 mm. The resulting gap is about 3.07 mm. The luminous length of the lamp is about 344 mm.

The gap of 3 mm is relatively wide in comparison to the penetration depth of UV-C waves into wine. To overcome this problem fluid guiding elements (FGE) were inserted modifying the flow in the gap. These FGE split the current into three separate laminar flow threads and guide them alternately to the lamp surface. The gap close to the UV-C lamp has a width of 0.6 mm the middle and the outer gap are 1.04 mm and 1.2 mm wide. The liquid is treated with UV-C energy when it flows through the 0.6 mm gap. There are seven FGE inside the reactor and each has a length of 60 mm (see Table 1).

The possible flow rates for the used reactor prototype are between 15 and 150 L/h. All these flow rates generate a laminar flow. The Reynolds numbers range between 101 and 1013 for the thin film reactor without the FGE. With the inserts the Reynolds number in the gap facing the lamp range between 37 and 371. The residence times for the TFR are

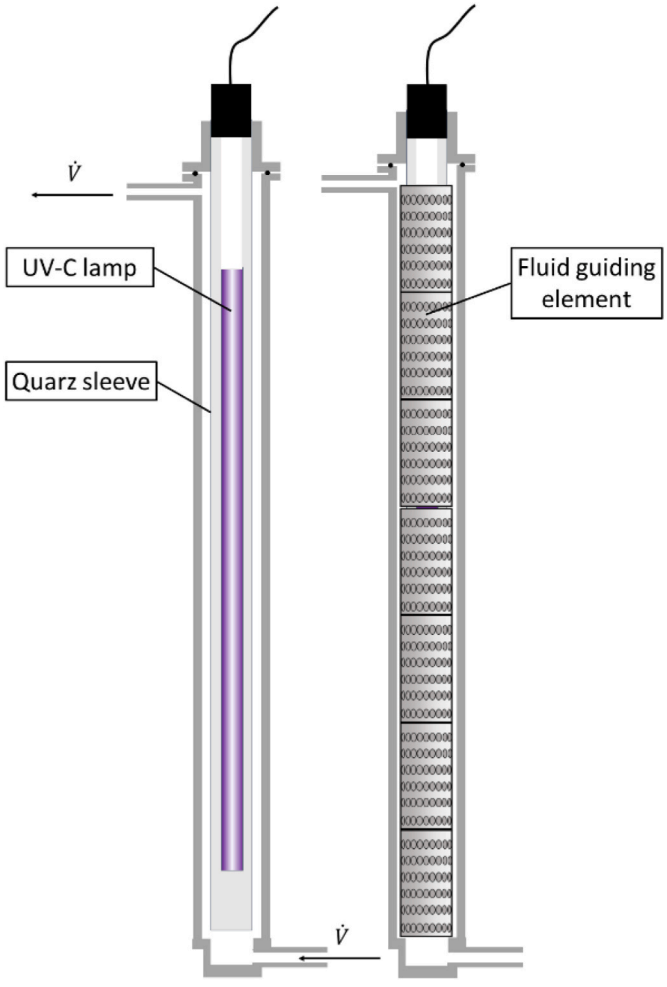

Fig. 1. Schematic drawing of the thin film reactor with a 3 mm gap (left) and the thin film reactor with flow guiding elements with a 0,6 mm gap (right). The reactor is flowed through from bottom to top.

between 3.6 ± 0.2 s and 33.1 ± 0,5 s and between 3.33 ± 0.2 s and 27.0 ± 0.4 s with inserted FGEs (Table 2). The reactor and the FGE are described in detail by Hirt et al. (2022).

2.2.2. Straight tube reactor ("serpentine reactor")

The "serpentine" reactor (Fig. 2) consists of 36 straight fluorethylenpropylen (FEP) tubes with an inner diameter of 6 mm and an outer diameter of 6.6 mm. Each tube has a length of 0.52 m which adds up to a total length of 20.98 m. The UV-C-transparency of the FEP tubes at 254 nm is 59 ± 3%. These tubes are connected through non-UV-transparent U-turns. Six 41 W low-pressure mercury lamps with an UV-C output of 16 W each are installed 300 mm above the FEP tubes. The flow can be adjusted between 30 L/h and 100 L/h. Resulting Reynolds numbers are between 1470 and 5826. The flow changes from laminar to turbulent at a Reynolds number of about 2400 (approx. 40 L/h). This was proven by measuring the dose required for the first log level inactivation at different Reynolds numbers. There is a sudden jump in the required dose at around Re = 2400 (Fig. 7).

2.2.3. Coiled tube reactor

This reactor (Fig. 3) has a FEP coiled tube of 23 m circulating around a 36 W low pressure mercury lamp (UVN30, UV-Technik Speziallampen GmbH, Germany). The FEP tube has an inner diameter d_i of 3.8 mm and an outer diameter of 4.6 mm. The inner diameter D of the coil is 38 mm and the length of the coil is about 750 mm. The critical Reynolds number Re_{crit} in a coiled tube can be calculated with Equation (2) (Verein Deutscher Ingenieure, 2010)

$$Re_{crit} = 2300\left[1 + 8.6\left(\frac{d_i}{D}\right)^{0,45}\right] \quad (2)$$

The critical Reynolds number for this reactor is 9212. The Reynolds number of the coiled tube reactor range from 971 at 10 L/h to 3780 at 40 L/h. Dean vortices appear when Reynolds numbers are smaller Re_{crit} and Dean numbers (De) exceed 54 (equation (3)).

$$De = Re * \sqrt{\frac{d_i}{D}} \quad (3)$$

The Dean numbers range from 294 to 1273 for 10 and 40 L/h, respectively. This results in Dean vortices, since the Dean number is greater 54 and the maximum Reynolds number (3,780) is below Re_{crit}.

2.2.4. Characteristic reactor settings for specific flow types

Specific reactor settings were chosen to investigate the influence of characteristic flow types on the inactivation of *S. cerevisiae* (Table 3).

2.2.5. Standard operating procedure for UV-C treatment

The following standard operating procedure (SOP) for UV-treatment procedure was applied for the microbiological inactivation as well as for the actinometry.

To ensure stable lamp performance the UV-C lamps had a warm up phase of 45 min before the experiment. To counteract a heating of the reactor during the warm up 20 °C tempered water was pumped through the reactor. During this time the flow rate was verified. The liquid was transferred in a sterile bottle and also tempered at 20 °C. The tube of the feeding peristaltic pump (Heidolph Hei-FLOW Precision 06) was sterilized with Bacillol® before pumping solution through the reactor. The first 150–400 mL of the liquid emerging the reactor were discarded. The amount was dependent on each reactor volume. At this point a steady state of the UV-C process is reached and a sample of 50 mL was taken while the remaining solution was collected in a sterile bottle. The treated liquid was then used as the new feeding solution and the process was repeated for each pass.

The cleaning of the reactor was carried out as follows. The reactor was flushed with 2 L of demineralized water and pumped empty. Afterwards 70% ethanol solution was pumped in circulation for about 10 min. After the reactor was pumped empty again it was once again flushed with 2 L demineralized water. The reactors were than blown dry with air for about 5 min. During the whole cleaning process the lamps were kept on. At regular intervals the reactors are additionally cleaned with a 0.1 Mol NaOH solution.

Table 1
Physical properties of the four wines used in this study.

Grape variety	A (254 nm,1 cm)	ρ [g/cm³]	NTU	pH	η [mPas]
Riesling	17.9 ± 1.1	0.9924 ± 0.0001	53 ± 9	3.3 ± 0.2	1.691 ± 0.015
Pinot Noir	34.9 ± 0.4	0.9910 ± 0.0001	103 ± 17	3.5 ± 0.2	1.867 ± 0.058
Carbernet Sauvignon Cuvée	45.1 ± 0.9 31.6 ± 0.8	0.9906 ± 0.0001 0.9904 ± 0.0001	50 ± 9 38 ± 2	3.8 ± 0.2 3.5 ± 0.2	1.91 ± 0.031 1.624 ± 0.002

Table 2
Comparison of the key figures of the reactors.

Reactor	Volume ccm	Flow L/h	Residence time s	Flowrate/ volume ratio 1/h	Re
TFR	147.5 ± 7.1	15–150	33.1–3.6	101.2–1016.9	101–1013
TFR + FGE	128.0 ± 6.2	15–150	27.0–3.3	117.2–1171.9	37–371
straight tube	604.9 ± 1.9	30–100	68.6–19.9	49.6–165.3	1470–5826
coiled tube	192.2 ± 1.0	10–40	68.8–17.3	52.0–208.1	971–3780

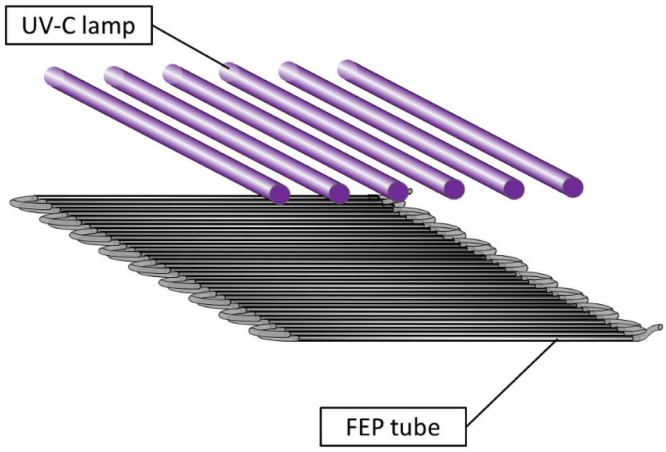

Fig. 2. Schematic drawing of the serpentine (straight tube) reactor.

2.3. Residence time distribution

The residence time distribution (RTD) F(t) shows the probability distribution of the time a particle is likely to spend in the reactor. A narrow distribution indicates good mixing within a reactor. The RTD is a way to characterize the performance of an UV-C reactors.

The RTDs were determined with a sodium chloride solution (Carl Roth GmbH + Co. KG, Karlsruhe, Germany) as a tracer. A step input was achieved by switching the inlet. The concentration at the outlet was measured via the conductivity. A conductivity sensor (FYA641LFP1, Ahlborn Mess-und Regelungstechnik GmbH, Holzkirchen, Germany) was detached to a data logger (Almemo 2690-8A, Ahlborn Mess-und Regelungstechnik GmbH, Holzkirchen, Germany). The conductivity was measured in 0.2 s intervals and normalized by the maximum

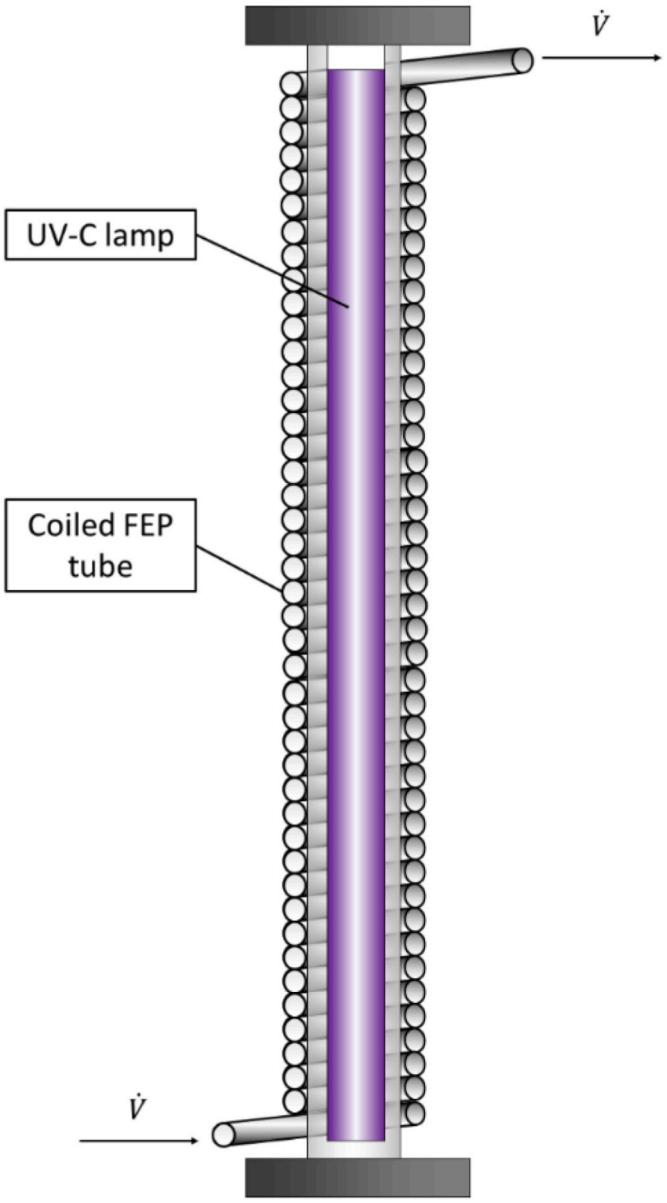

Fig. 3. Schematic drawing of the coiled tube (Dean vortex) reactor. The reactor is flowed through from bottom to top.

Table 3
Investigated flow types and the reactor settings to reach them.

Flow type	Reactor	Flow rate L/h	Re	Re_{crit}	De	Color in paper
Laminar thin film 3 mm	TFR	100	675	2300	–	Dark blue
Laminar thin film 0,6 mm (FGE)	TFR + FGE	100	247[a]	2300	–	Light blue
Laminar tube flow	Serpentine	30	1879	2300	–	Yellow
Turbulent tube flow	Serpentine	100	6263	2300	–	Red
Dean-Vortex	Coiled tube	40	3680	9212	1273	Green

[a] In the 0.6 mm gap facing the UV-C source.

measured conductivity value.

The mean residence time τ was determined by

$$\tau = \int_0^1 t\, dF(t) = \int_0^1 t\, E(t)\, dt \tag{4}$$

where E(t) is the residence time sum function. To compare the different reactors the RTD was plotted as a function of the normalized time $F(\Theta = t/\tau)$.

The Bodenstein number is a way to quantify and compare the RTDs with a dimensionless figure. It is defined as the ratio of the convection flow to the dispersion flow. The Bodenstein number allows statements about how much volume elements or substances within a reactor mix due to the prevalent currents. The reactors can be considered open at both ends. Therefore the RTD can be described by the analytically solved dispersion model displayed in equations (5) and (6) (Levenspiel, 1999, p. 3).

$$E(Bo) = \frac{1}{2}\sqrt{\frac{Bo}{\pi \cdot \Theta}} \cdot \exp\left(-\frac{(1-\Theta)^2 Bo}{4\Theta}\right); \quad for\ Bo > 100 \tag{5}$$

$$E(Bo) = \frac{1}{2}\sqrt{\frac{Bo}{\pi \cdot \Theta}} \cdot \exp\left(-\frac{(1-\Theta)^2 Bo}{4}\right); \quad for\ Bo < 100 \tag{6}$$

The Bodenstein number was determined by fitting $E(Bo)$ to $E(t)$. The fit was made to minimize the sum of the errors squared using the solver function of MS-Excel. Each RTDs was measured threefold. The mean and standard deviation were calculated for each flow type.

The qualtity of the fits was determined by calculating the coefficient of determination R^2.

$$R^2 = 1 - \frac{\sum_i \left(x_{i,measured} - x_{i,fit}\right)^2}{\sum_i \left(x_{i,measured} - \overline{x}_{mean,measured}\right)^2} \tag{7}$$

The Bodenstein number was then used to calculate the variance σ_θ^2 of $E(\Theta)$ with equations (8) and (9)

$$\sigma_\theta^2 = \frac{2}{Bo}; \quad for\ Bo < 100 \tag{8}$$

$$\sigma_\theta^2 = \frac{2}{Bo} + \frac{8}{Bo^2}; \quad for\ Bo > 100 \tag{9}$$

σ_Θ shows the deviation of the residence time from the mean residence time. And there for the deviation of an ideal plug flow.

2.4. Actinometry

This study aims to show the differences in the dose response of *S. cerevisiae* dependent on the flow type. Therefore, a biodosimetrical approach to quantify the UV-C dose is not valid. Instead the total amount of UV-C energy absorbed by the liquid is to be determined. To achieve this, the iodide/iodate actinometer developed and described by R. O. Rahn (1997) was used. This chemical actinometer quantifies the transformation from iodide to triiodide photometrically at 352 nm. The reaction is as follows:

$$8\ KI + KIO_3 + 3\ H_2O + h\nu \rightarrow 3\ I_3^- + 6\ OH^- + 9\ K^+ \tag{10}$$

solution of 0.6 *M* iodide and 0.1 *M* iodate in 0.01 *M* borate buffer (pH 9.25) was used.

2.5. Investigation of microbial inactivation

Saccharomyces cerevisiae (EATON SIHA® Aktivhefe 7 (Rieslinghefe) *Sacharomyces cerevisiae*, strain D 576) was grown in YPD nutrient broth on a shaking incubator (90 rpm) for 24 h at 30 °C. The nutrient broth with *S. cerevisiae* was centrifuged, decanted and transferred into ringer

solution. The initial cell count in the broth was determined by measuring the optical density (OD) at 600 nm. The model medium was inoculated with approximately 10^6 CFU/mL. The media were treated with UV-C energy according to the SOP.

In order to determine microbial counts, the UV-C treated medium was diluted in tenfold dilution series in 0.9% NaCl and plated out. A YPD agar with antibiotics (25 μg/ml Kanamycin and 30 μg/ml Chloramphenicol) was used as the culture medium. The inoculated plates were incubated at 30 °C for 48 h and then colonies were counted. All microbial count determinations were done in triplicates.

The inactivation curve of this *S. cerevisiae* has a shoulder. Such curves can be described with the Weibull- and Chick-Watson-model (Atilgan et al., 2021).

In the present study the equations have been modified so that they are dependent on the UV-C-dose D_{UV} instead of the exposure time. The Weibull model is defined as

$$\log\left(\frac{N}{N_o}\right) = -\left(\frac{D_{UV}}{\delta}\right)^p \tag{11}$$

Where δ is the UV-C dose acquired for the first order of inactivation, p is the shape parameter and describes downward concavity $(p > 1)$ or upward concavity $(p < 1)$ of the curve (if $p = 1$, curve is linear).

The Chick-Watson Model is defined as

$$\log\left(\frac{N}{N_0}\right) = k(1 - \exp(-k_1 \cdot D_{UV})) \tag{12}$$

Where k and k_1 are the inactivation rate constants for linear part and tailing or shoulder region, respectively (Marugán et al., 2008).

2.6. Model solution

Wine has a complex matrix whose ingredients depend on many factors such as vine, origin, season or production process and therefore can vary. To minimize these influencing factors, a model solution was used. The model solution aims to simulate the optical properties of wine and should not supply nutrients for the organisms. Otherwise the processing time from inoculation to plating could impact the cell count. Thus, we decided for a ringer solution dyed with "sunset yellow", an azo-dye used for coloring food. The dye itself shows no effect on the organisms and does not change due to the UV-C treatment. The extinction at 254 nm was measured before and after inoculation.

In this paper the term absorbance is only used for solutions or rather the effect of the dissolved dye and therefore the liquid before inoculation. The term OD describes the extinction of the dispersion after inoculation the liquid with microorganisms. The OD as well as the absorbance are decadic.

3. Results and discussion

3.1. Residence time distribution (RTD)

Since the penetration depth of UV-C light into liquid food is usually shorter than the reactor dimensions it is imperative to interchange the portion of the treated liquid that is facing the UV-C source. Otherwise only a fraction of the volume is treated, while the rest of the liquid is not affected by the UV-C light. Therefore, an ideal plug flow with turbulences that interchanges the volume with convection of the vortices should provide the best results.

The dispersion model and Bodenstein number are only suitable for the characterization of the UV-C reactors to a limited extent. However, it provides a single key figure to describe the shape of the RTD. Therefore, a quantitative comparison between reactors in this study, as well as in future studies is simplified. σ_Θ in Table 4 shows the non-uniformity of the residence time. A narrow distribution would be favorable, since all volume fractions are treated almost uniformly. As expected the turbulent flow hast the narrowest distribution, followed by the dean vortices. The three laminar flow types have much broader distributions (Fig. 4).

Table 4
Evaluation of the residence time distribution. Means of the Bodenstein number Bo, the standard deviation σ_Θ and the Coefficient of determination R^2 and their deviation.

Flow type	Bo	σ_Θ	R^2
laminar tube flow	80.5 ± 2.2	0.157 ± 0.002	> *0,99*
turbulent tube flow	2353.3 ± 343.1	0.029 ± 0.002	> *0,99*
Dean vortex flow	646.3 ± 30.0	0.056 ± 0.001	> *0,99*
laminar thin film 3 mm	25.4 ± 0.8	0.275 ± 0.004	> *0,99*
laminar thin film 0,6 mm	66.3 ± 9.8	0.174 ± 0.011	> *0,99*

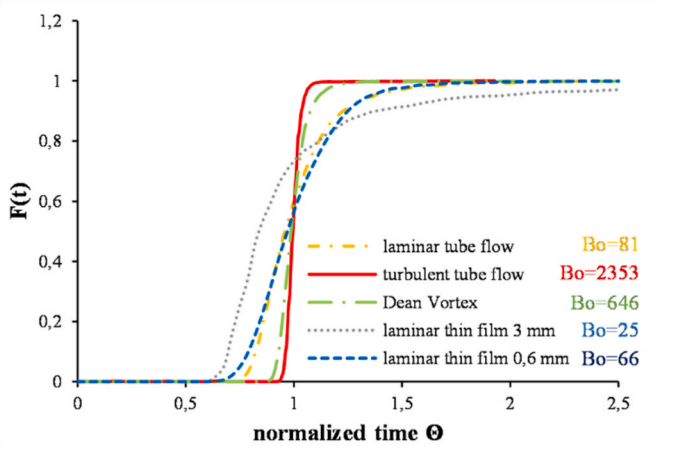

Fig. 4. Comparison of the residence time distribution and the calculated Bodenstein number for the different flow types/reactor settings.

3.2. UV-C dose comparison

To quantify the UV-energy input of each reactor the iodide/iodate actinometer was used to measure the actinometric dose D_{act} at various flow rates $\dot{V}$.

The iodide/iodate actinometer reaches its limit in laminar condition. Since the absorbance of the actinometric solution at 254 nm is very high (~180 cm^{-1}) only the boundary layer next to the source is treated with UV-C energy. This liquid layer is practically not exchanged in laminar flow. The photochemical reaction reaches its limit. Therefore, the actinometric measurements do not reflect the total amount of absorbed UV-energy. The quantum yield of the photochemical reaction is stable when for iodide concentrations from 0.6 Mol to 0.1 Mol. The difference is only 6% (R. Rahn et al., 2003). If the iodide concentration drops below the 0.1 Mol the quantum yield decreases drastically. This iodide depletion happens locally in the volume fraction near the lamp. Hirt et al. (2022) proved that this is not the case for the actinometric solution as a whole. This becomes obvious when looking at the resulting actinometric UV-C power in Fig. 5. Power seems to increase with flow rates. However, power should be constant for each reactor, since their lamps are not affected by changing flow rates.

$$P_{UVC,act} = \frac{D_{act}}{\dot{V}} \tag{13}$$

Here, b is a shape parameter and OS is the offset of the flow rate. The offset is necessary because the curve should not run through the zero point. $P_{UVC,max}$ is given in W and $\dot{V}$ in h/L.

$P_{UVC,max}$ was used to calculate the dose D_{calc} at a given flow rate.

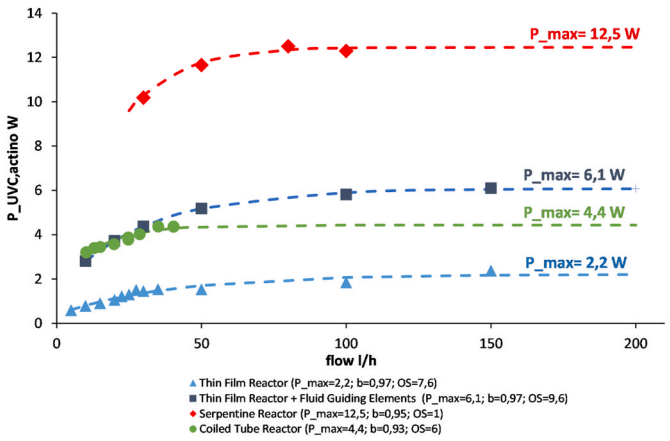

Fig. 5. Actinometrically measured UVC power over flow rate. The dotted lines are fits in form of equation (14). The parameter are listed in the legend.

$$P_{UVC,act} = P_{UVC,max}\left(1 - b^{(\dot{V}+OS)\cdot\frac{k}{L}}\right) \quad (14)$$

Therefore, the maxima that are reached asymptotically by the data plotted for each reactor in Fig. 5 represent the actual UV-C power effecting the treated liquids. An empirical fit was made for the power values measured by actinometry ($P_{UVC,act}$) to calculate the limit and thus the actual UV-C power ($P_{UVC,max}$) by each reactor (Eq. (13)).

$$D_{calc} = P_{UVC,max}\cdot\dot{V} \quad (15)$$

The thin film reactor should yield the same power independent of the inserts. Therefore, the $P_{UVC,max}$ of the TFR with FGE of 6.1 W is also used to calculate the dose of the TFR without the FGE. The estimated UV-C power ($P_{UVC,max}$) and calculated dose (D_{calc}) of the reactor settings for the flow types are listed in Table 5.

3.3. Inactivation of Saccharomyces cerevisiae

S. cerevisiae was chosen as an exemplary main organism, because it is easy to handle and proved to be less sensitive to UV-C treatment than most other organisms in wine in pilot tests (Diesler et al., 2019).

3.3.1. Modeling the inactivation curve

There are many models for the inactivation curves of microorganisms. Other studies show, the inactivation of *S. cerevisiae* shows either a shoulder or a log-linear characteristic. Sommer et al. (1996) show a similar shoulder for the UV-C inactivation of *S. cerevisiae* strains (RC43a and a wild type) that are similar to the observed *S. cerevisiae D576* (Fig. 6). They also found strains with a log-linear inactivation (YNN281 and YNN282). Junqua et al. (2020) studied the inactivation of *S. cerevisiae* FX10 in wine and also detected a shoulder. Feliciano et al. (2019) observed the same shoulder for *S. cerevisiae* BFE-39 in orange juice. Only Feliciano et al. (2019) applied an inactivation model to their results. The used model was developed by Baranyi and Roberts (1994) to original predict growth of bacteria in food and not the inactivation of yeast.

Table 5
Actinometric dose of one pass through each reactor with the used reactor settings for characteristic flow types.

Flow type	$P_{UVC,max}$ W	D_{calc} J/L
Laminar thin film 3 mm	6.1 ± 0,2	218
Laminar thin film 0,6 mm (FGE)	6.1 ± 0,2	218
Laminar tube flow	12.5 ± 0.3	1495
Turbulent tube flow	12.5 ± 0.3	449
Dean-Vortex	4.4 ± 0.2	398

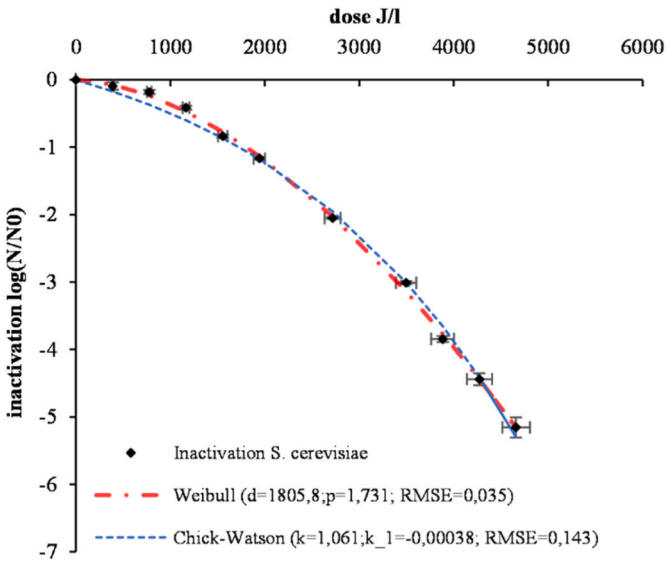

Fig. 6. Inactivation curve of *Saccharomyces cerevisiae* in a model solution with OD 43 in a coiled tube Dean Vortex reactor; 12 passes through the reactor. Comparison of Weibull and Chick-Watson model.

More recently, Atilgan et al. (2021) list commonly used models for UV inactivation of several microorganisms in general. Here, the Weibull model and the Chick-Watson model both describe a kinetic with a shoulder as seen for *S. cerevisiae* D576 (Fig. 6). Overall the Weibull Models shown a better fit (lower RMSE) than the Chick-Watson model.

In Fig. 7 the δ of the serpentine reactor is shown dependent on the Reynolds number. Since the only parameter that changed during this experiment was the flow velocity and therefor the Reynolds number, the sudden drop of the dose needed for the first log inactivation is prove of the turnover point from laminar to turbulent flow at a Reynolds number around 2400 as suggested in 2.2.2.

3.3.2. Verifying the model solution

Wine is a complex matrix which comprises at least three major parameters that could impact the inactivation of *S. cerevisiae*.: absorbance, pH and ethanol content.

The influence of ethanol on the UV inactivation of *S. cerevisiae* was varied as well as the pH-level in a wine typical range. There was no significant ($\alpha = 0.05$) change in the inactivation dependent on the ethanol content and pH-level as seen in Figs. 8 and 9, respectively. The different compositions were carried out in triplets. Gouma et al. (2015) studied the inactivation of *S. cerevisiae STCC 1172* in apple juice and did not find a significant (Excel ANOVA $\alpha = 0,05$) change in inactivation by

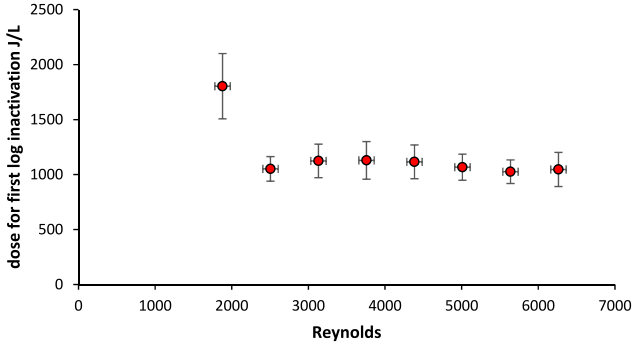

Fig. 7. Dose for the first log inactivation δ dependent on the Reynolds number in the serpentine reactor.

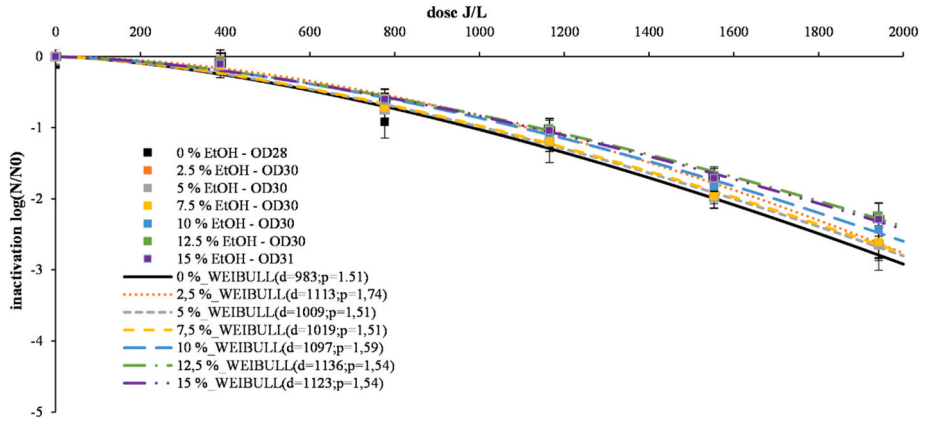

Fig. 8. Inactivation curves for *S. cerevisiae* dependent on the ethanol concentration in Dean vortices with their respective Weibull functions.

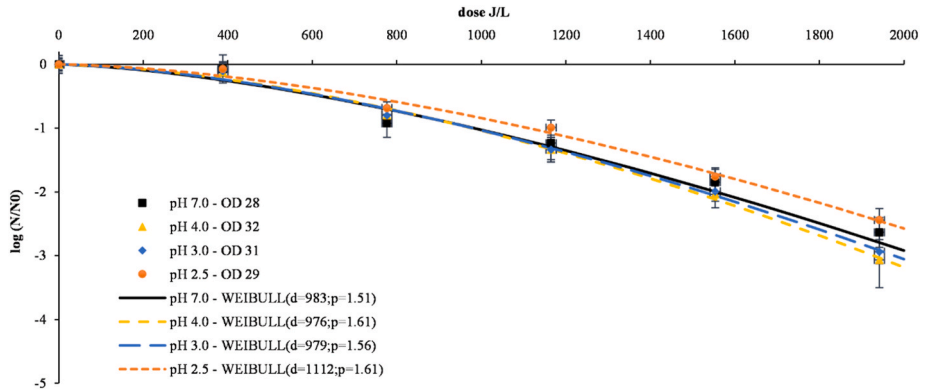

Fig. 9. Inactivation curves for *S. cerevisiae* dependent on the pH level in a model solution in Dean vortices with their respective Weibull functions.

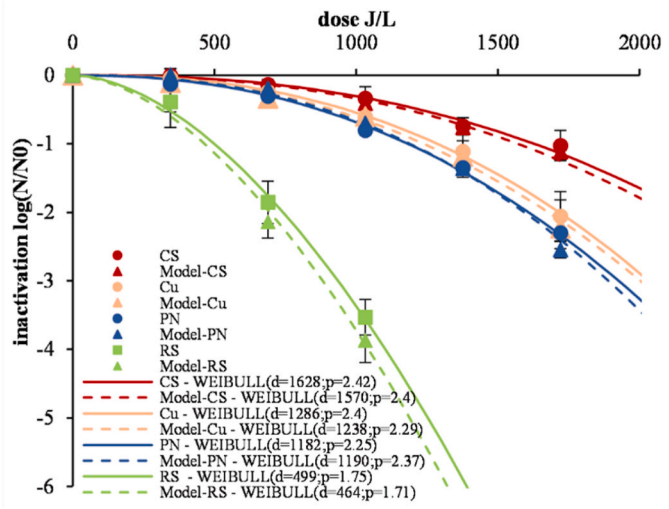

Fig. 10. Comparison of inactivation in wine and their respective model solution in turbulent flow (CS: cabernet sauvignon; Cu: cuvée, PN: pinot noir, RS: Riesling. Weibull functions are plotted accordingly.

varying the pH-value between 3.0 and 7.0 with McIlvaine buffer.

It is not necessary to adjust the ethanol content or the pH-value to emulate the UV-C inactivation of *S. cerevisiae* in wine. Fig. 10 shows a comparison of the inactivation in Cabernet Sauvignon, Pinot Noir, red wine cuvée, Riesling and their respective model solutions consisting of ringer solution and sunset yellow. The deviations between the wines and their model solutions are not significant ($\alpha = 0.05$).

Thus, the mixture of ringer solution and sunset yellow is a viable model to imitate the inactivation of *S. cerevisiae* in real wine.

3.3.3. Modeling the dependence of OD and flow type

For each flow type between 15 and 25 inactivation curves were recorded with optical densities of model solutions between 0 and 50. For most experiments at least six passes through the respective reactors were conducted. For each inactivation curve the Weibull model was fitted and the δ and p parameters were determined. Inactivation curves with less than four valid datapoints were discarded. This was usually the case for samples with an OD lower than 10, were the inactivation falls below the detection limit after a few passes through the reactor. In cases were the inactivation did not reach the first log-level in the observed dose range, the parameters were disregarded as well. For inactivation that exceeded the first log-level but not the third one, only the δ and not p parameters were accepted.

The δ parameter has a strong correlation to the OD of the treated solutions. There are also differences in these correlations dependent on the flow type. A linear equation for $\delta(OD)$ was fitted for each flow type (Table 6).

Table 6
Linear fits for the Weibull δ parameter depended on the optical density (OD).

Flow type	$\delta(OD)$	R^2
Laminar thin film 3 mm	$202,3 + 79,5 \cdot OD$	0,89
Laminar thin film 0,6 mm (FGE)	$179,5 + 25,2 \cdot OD$	0,91
Laminar tube flow	$56,3 + 109,0 \cdot OD$	0,86
Turbulent tube flow	$41,9 + 28,1 \cdot OD$	0,95
Dean-Vortex	$34,0 + 31,7 \cdot OD$	0,90

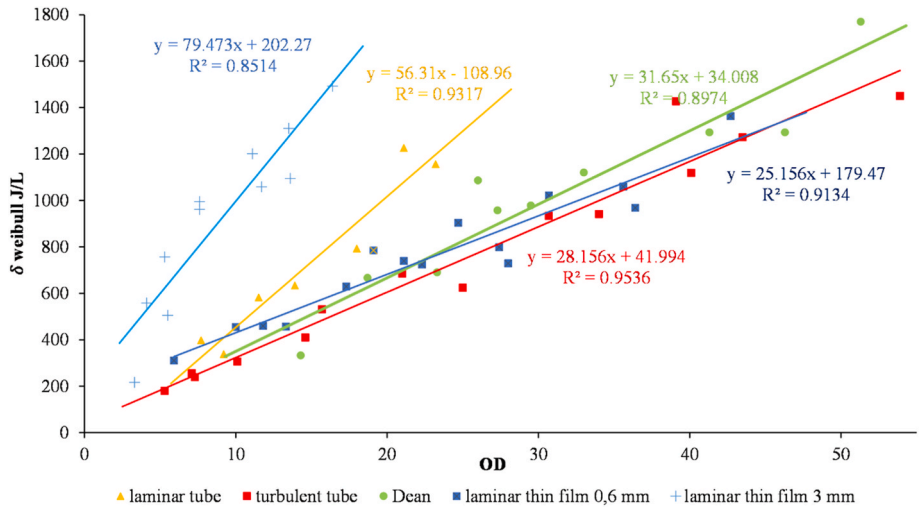

Fig. 11. The delta Weibull parameter fit for the different flow types.

These linear equations are plotted in Fig. 11.

The δ parameter for the laminar thin film 3 mm shows by far the highest dose required for the reduction of the first log level. Gouma et al. (2015) used a similar annular thin film reactor with a 2.5 mm gap for the inactivation of *S. cerevisiae* (STCC 1172, STCC 1170, STCC11034 and STCC1996). Here, in a McIlvaine buffer model solution with an absorbance of 10.7 a dose between 1200 J/L and 2000 J/L was needed for the first log level reduction of the different yeast strains which is broadly in the range that can be predicted with the presented model for a similar reactor design

In contrast to the δ parameter the shape parameter p shows no correlation to the OD. However, there is a dependence on the flow type as seen in Fig. 12.

At this state it is unknown if the p-factor has a correlation to any other process parameter. Therefore, the p factors were averaged for each different flow type. The results are shown in Table 7. The p factor of the Dean-Vortex and the laminar thin film 3 mm is significantly ($\alpha = 0,05$) lower than the factor for the other flow types. The higher the value, the faster the inactivation progress.

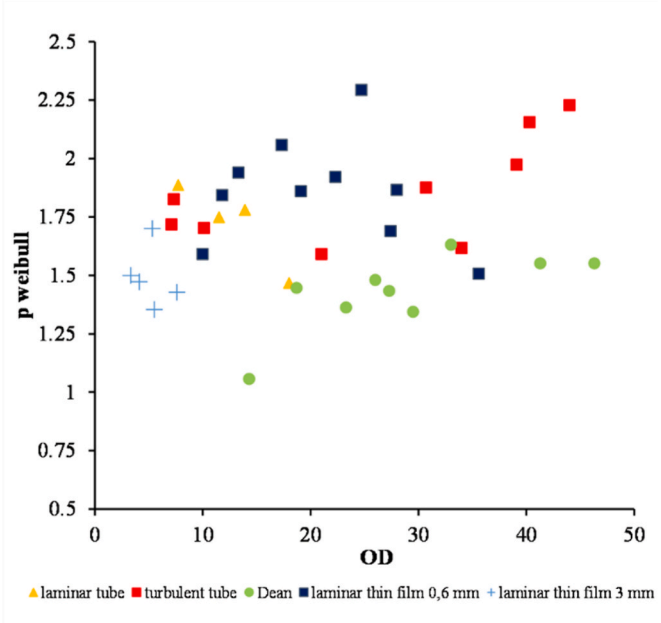

Fig. 12. Weibull p-parameters over the OD. Flow types are colored accordingly.

Table 7
Mean values of the Weibull p parameter for the different flow types.

flow type	*p*
Turbulent tube flow	$1.85 \pm 0,23$
Laminar tube flow	$1,81 \pm 0,23$
Dean-Vortex	$1,34 \pm 0,17$
Thin film 0,6 mm	$1.86 \pm 0,23$
Thin film 3 mm	$1.49 \pm 0,13$

With these parameters the inactivation of *S. cerevisiae* in the investigated model wine solutions can be predicted with the Weibull model for each flow type:

Turbulent tube flow:

$$log\left(\frac{N}{N_o}\right) = -\left(\frac{D}{28,2 \cdot OD_{254nm} + 42,0}\right)^{1,85} \tag{16}$$

laminar tube flow:

$$log\left(\frac{N}{N_o}\right) = -\left(\frac{D}{56,3 \cdot OD_{254nm} + 109,0}\right)^{1,81} \tag{17}$$

Dean Vortex:

$$log\left(\frac{N}{N_o}\right) = -\left(\frac{D}{31,7 \cdot OD_{254nm} + 34,0}\right)^{1,43} \tag{18}$$

Laminar thin film 0,6 mm:

$$log\left(\frac{N}{N_o}\right) = -\left(\frac{D}{25,2 \cdot OD_{254nm} + 179,4}\right)^{1,86} \tag{19}$$

Laminar thin film 3 mm:

$$log\left(\frac{N}{N_o}\right) = -\left(\frac{D}{79,5 \cdot OD_{254nm} + 202,3}\right)^{1,49} \tag{20}$$

The deviation for the predictions can be calculated with Gaussian error propagation (Equation (21)). The deviation σ_δ was estimated to be 5%

$$\sigma_{log\left(\frac{N}{N_0}\right)} = \sqrt{\left(\frac{p\left(D/\delta\right)^p}{\delta} \cdot \sigma_\delta\right)^2 + \left(ln\left(\frac{D}{\delta}\right) \cdot \left(\frac{D}{\delta}\right)^p \cdot \sigma_p\right)^2} \tag{21}$$

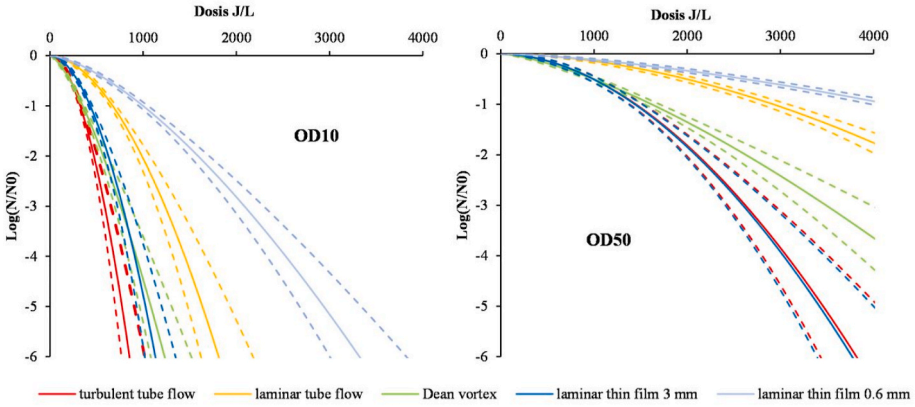

Fig. 13. Predicted inactivation of *S. cerevisiae* for the different flow type with different optical densities of the treated solution at optical densities of OD10 (left) and OD50 (right). Dotted lines are deviations.

Fig. 13 shows predictions for the inactivation of *Saccharomyces cerevisiae* at OD10 and OD50 dependent on the flow type. The thin film 3 mm and the laminar tube flow show the worst dose response of the studied flow types. At lower optical densities the Dean Vortex, the 0,6 mm thin film and the turbulent tube flow show comparable results with each other. With the increase of the optical density the Dean Vortex shows an inferior dose response to the turbulent flow and the 0,6 mm thin film. This relation can be displayed by rearranging the model so that a given inactivation is assumed. Often times a 5-log reduction is considered as a sufficient inactivation. The FDA for example used the 5-log reduction of *E. coli 0157:H7* to approve the cidersure® reactors (FPE, Inc., Rochester, NY).

Fig. 14 shows the dose required for a 5-log inactivation dependent on the optical density and for each flow type. *S. cerevisiae* is less UV sensitive than *E. coli* but the correlations are the same.

The efficiency of the inactivation correlates with the rate at which the medium facing the lamp is interchanged. The Bodenstein number is an indicator for the mixing in the reactor. Since mixing is required to exchange the liquid facing the lamp, the Bodenstein number should be an indicator for the effectiveness of the inactivation in a UV reactor especially in opaque liquids where the penetration depth is relatively short. Our findings confirm this theory with one exception: The laminar thin film flow 0.6 mm. This is due to the fact, that the difference of the gap width and the penetration depth is not as big as within the other reactors. Fig. 13 shows that the turbulent tube flow and the laminar thin film 0.6 mm show the best inactivation in opaque liquids like red wine (OD20 – OD50) followed by Dean Vortices. As expected, the laminar flow in a thin film (3 mm) and a tube with a dimension much larger than the penetration depth show the slowest inactivation kinetic similar to no mixing at all as shown with residence time distribution (RTD). In less absorbent liquids (OD < 10) the penetration depth exceeds the gap of the fluid guiding elements. A part of the radiation goes through the liquid and hits the wall of the channel without being effectively used for inactivation of microorganisms. Therefore, the turbulent flow causes a more efficient inactivation than the laminar thin film 0.6 mm at low optical densities.

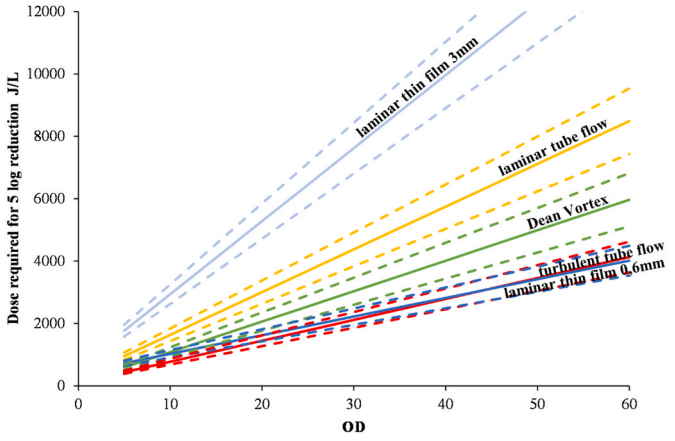

Fig. 14. Required UV-C dose for a 5-log reduction of *S. cerevisiae* D 576 dependent on the optical density of the wine model solution and the flow type with deviations (dotted lines).

4. Conclusions

The model solution consisting of ringer solution and sunset yellow is an adequate substitute to investigate the inactivation of *Saccharomyces cerevisiae* in wine as shown with Cabernet Sauvignon, Pinot Noir, red wine cuvée and Riesling.

This study shows that there is not just one dose-response-relation for organisms in opaque liquid food. Beside the absorbance of the liquid, the flow type has a huge impact on the inactivation. As shown by the modelled Weibull-formula. The best overall efficacy of inactivation in the observed parameter range is reached with a turbulent flow. Compared to this, the inactivation in a Dean Vortex flow system is less efficient. The inactivation in a laminar flow is the least efficient. This was to be expected, since vortices are needed to interchange the portion of the volume directly facing the UV-C source. However, there is the exception of the annular thin film reactor with flow guiding elements. When the absorbance of the treated medium is greater than 20, like a red wine, the guided laminar flow is as effective as the turbulent flow in inactivating *S. cerevisiae*. If the absorbance is below 20 the inactivation is slightly inferior to the turbulent flow.

Funding

This work was supported by the Research Association of the German Food Industry (FEI) (Project number: AiF 20921 N).

Declaration of interest

All authors declare that they do not have any conflict of interest.

CRediT authorship contribution statement

Benedikt Hirt: Writing – original draft, Data curation, Formal analysis, Visualization, Investigation, Conceptualization, Project administration. **Jaayke Fiege:** Writing – review & editing. **Svetlana Cvetkova:** Writing – review & editing. **Volker Gräf:** Writing – review & editing, Conceptualization, Funding acquisition. **Maren**

Scharfenberger-Schmeer: Writing – review & editing, Funding acquisition. **Dominik Durner:** Writing – review & editing, Funding acquisition. **Mario Stahl:** Writing – review & editing, Funding acquisition, Supervision, Conceptualization.

Declaration of competing interest

The authors declare that there is no financial/personal interest or belief that could affect our objectivity.

Data availability

Data will be made available on request.

Acknowledgements

We thank Claudia Csovcsics, Josanna Kaufmann, Veronika Larche and Annemarie Regier for their excellent technical assistance. We thank Jürgen Heinrich, Reiner Seitz and Ralph Seelig for building the prototype reactors. We thank Andreas Hensel and the IMVT of the KIT for the provision of the FGE.

Abbreviations Used

Bo	Bodenstein number
De	Dean number
FGE	Fluid guiding element
OD	optical density
SD	standard deviation
Re	Reynolds number
RMSE	Root-mean-square deviation
RTD	Residence time distribution
TFR	Thin Film Reactor
UV	ultraviolet;

References

Atilgan, M. R., Yildiz, S., Kaya, Z., & Unluturk, S. (2021). Kinetic and process modeling of UV-C irradiation of foods. In K. Knoerzer, & K. Muthukumarappan (Eds.), *Innovative food processing technologies: A comprehensive review* (pp. 227–255). Elsevier. https://doi.org/10.1016/B978-0-08-100596-5.22972-7.

Baranyi, J., & Roberts, T. A. (1994). A dynamic approach to predicting bacterial growth in food. *International Journal of Food Microbiology, 23*(3–4), 277–294. https://doi.org/10.1016/0168-1605(94)90157-0

Barut Gök, S. (2021). UV-C treatment of apple and grape juices by modified UV-C reactor based on dean vortex Technology: Microbial, physicochemical and sensorial parameters evaluation. *Food and Bioprocess Technology, 14*(6), 1055–1066. https://doi.org/10.1007/s11947-021-02624-z

Baykuş, G., Akgün, M. P., & Unluturk, S. (2021). Effects of ultraviolet-light emitting diodes (UV-LEDs) on microbial inactivation and quality attributes of mixed beverage made from blend of carrot, carob, ginger, grape and lemon juice. *Innovative Food Science & Emerging Technologies, 67*, Article 102572. https://doi.org/10.1016/j.ifset.2020.102572

Buzrul, S. (2012). High hydrostatic pressure treatment of beer and wine: A review. *Innovative Food Science & Emerging Technologies, 13*, 1–12. https://doi.org/10.1016/j.ifset.2011.10.001

Costanigro, M., Appleby, C., & Menke, S. D. (2014). The wine headache: Consumer perceptions of sulfites and willingness to pay for non-sulfited wines. *Food Quality and Preference, 31*, 81–89. https://doi.org/10.1016/j.foodqual.2013.08.002

Crook, J. A., Rossitto, P. V., Parko, J., Koutchma, T., & Cullor, J. S. (2015). Efficacy of ultraviolet (UV-C) light in a thin-film turbulent flow for the reduction of milkborne pathogens. *Foodborne Pathogens and Disease, 12*(6), 506–513. https://doi.org/10.1089/fpd.2014.1843

Diesler, K., Golombek, P., Kromm, L., Scharfenberger-Schmeer, M., Durner, D., Schmarr, H.-G., Stahl, M. R., Briviba, K., & Fischer, U. (2019). UV-C treatment of grape must: Microbial inactivation, toxicological considerations and influence on chemical and sensory properties of white wine. *Innovative Food Science & Emerging Technologies, 52*, 291–304. https://doi.org/10.1016/j.ifset.2019.01.005

Feliciano, R. J., Estilo, E. E. C., Nakano, H., & Gabriel, A. A. (2019). Ultraviolet-C resistance of selected spoilage yeasts in orange juice. *Food Microbiology, 78*, 73–81. https://doi.org/10.1016/j.fm.2018.10.003

Fenoglio, D., Ferrario, M., Schenk, M., & Guerrero, S. (2020). Effect of pilot-scale UV-C light treatment assisted by mild heat on E. Coli, L. Plantarum and S. Cerevisiae inactivation in clear and turbid fruit juices. Storage study of surviving populations. *International Journal of Food Microbiology, 332*, Article 108767. https://doi.org/10.1016/j.ijfoodmicro.2020.108767

Giorges, A. T. G., Pierson, J. A., & Forney, L. J. (2008). Effect of reactor length on the disinfection of fluids in Taylor¬Couette photoreactor. *Industrial & Engineering Chemistry Research, 47*(19), 7490–7495. https://doi.org/10.1021/ie800250r

Golombek, P., Wacker, M., Buck, N., & Durner, D. (2021). Impact of UV-C treatment and thermal pasteurization of grape must on sensory characteristics and volatiles of must and resulting wines. *Food Chemistry, 338*, Article 128003. https://doi.org/10.1016/j.foodchem.2020.128003

Gouma, M., Gayán, E., Raso, J., Condón, S., & Álvarez, I. (2015). Inactivation of spoilage yeasts in apple juice by UV–C light and in combination with mild heat. *Innovative Food Science & Emerging Technologies, 32*, 146–155. https://doi.org/10.1016/j.ifset.2015.09.008

Hirt, B., Hansjosten, E., Hensel, A., Gräf, V., & Stahl, M. (2022). Improvement of an annular thin film UV-C reactor by fluid guiding elements. *Innovative Food Science & Emerging Technologies, 77*, Article 102988. https://doi.org/10.1016/j.ifset.2022.102988

Junqua, R., Vinsonneau, E., & Ghidossi, R. (2020). Microbial stabilization of grape musts and wines using coiled UV-C reactor. *OENO One, 54*(1). https://doi.org/10.20870/oeno-one.2020.54.1.2944

Koutchma, T. (2008). UV light for processing foods. *Ozone: Science & Engineering, 30*(1), 93–98. https://doi.org/10.1080/01919510701816346

Koutchma, T., & Parisi, B. (2004). Biodosimetry of Escherichia coli UV inactivation in model juices with regard to dose distribution in annular UV reactors. *Journal of Food Science, 69*(1), FEP14–FEP22. https://doi.org/10.1111/j.1365-2621.2004.tb17862.x

Koutchma, T., Popović, V., Ros-Polski, V., & Popielarz, A. (2016). Effects of ultraviolet light and high-pressure processing on quality and health-related constituents of fresh juice products. *Comprehensive Reviews in Food Science and Food Safety, 15*(5), 844–867. https://doi.org/10.1111/1541-4337.12214

Levenspiel, O. (1999). *Chemical reaction engineering.* Wiley. https://books.google.de/books?id=vw48EAAAQBAJ.

Marugán, J., van Grieken, R., Sordo, C., & Cruz, C. (2008). Kinetics of the photocatalytic disinfection of Escherichia coli suspensions. *Applied Catalysis B: Environmental, 82*(1–2), 27–36. https://doi.org/10.1016/j.apcatb.2008.01.002

Morata, A., Benito, S., González, M. C., Palomero, F., Tesfaye, W., & Suárez-Lepe, J. A. (2012). Cold pasteurisation of red wines with high hydrostatic pressure to control dekkera/brettanomyces: Effect on both aromatic and chromatic quality of wine. *European Food Research and Technology, 235*(1), 147–154. https://doi.org/10.1007/s00217-012-1742-7

Müller, A., Stahl, M. R., Greiner, R., & Posten, C. (2014). Performance and dose validation of a coiled tube UV-C reactor for inactivation of microorganisms in absorbing liquids. *Journal of Food Engineering, 138*, 45–52. https://doi.org/10.1016/j.jfoodeng.2014.04.013

Ngadi, M., Smith, J. P., & Cayouette, B. (2003). Kinetics of ultraviolet light inactivation of Escherichia coli O157:H7 in liquid foods. *Journal of the Science of Food and Agriculture, 83*(15), 1551–1555. https://doi.org/10.1002/jsfa.1577

Pendyala, B., Patras, A., Sudhir Gopisetty, V. V., & Sasges, M. (2021). UV-C inactivation of microorganisms in a highly opaque model fluid using a pilot scale ultra-thin film annular reactor: Validation of delivered dose. *Journal of Food Engineering, 294*, Article 110403. https://doi.org/10.1016/j.jfoodeng.2020.110403

Puértolas, E., López, N., Condón, S., Álvarez, I., & Raso, J. (2010). Potential applications of PEF to improve red wine quality. *Trends in Food Science & Technology, 21*(5), 247–255. https://doi.org/10.1016/j.tifs.2010.02.002

Rahn, R. O. (1997). Potassium iodide as a chemical actinometer for 254 nm radiation: Use of Iodate as an electron scavenger. *Photochemistry and Photobiology, 66*(4), 450–455. https://doi.org/10.1111/j.1751-1097.1997.tb03172.x

Rahn, R., Stefan, M. I., Bolton, J. R., Goren, E., Shaw, P.-S., & Lykke, K. R. (2003). Quantum yield of the iodide–iodate chemical actinometer: Dependence on wavelength and concentration. *Photochemistry and Photobiology, 78*(2), 146. https://doi.org/10.1562/0031-8655(2003)0780146QYOTIC2.0.CO2

Sommer, R., Haider, T., Cabaj, A., Heidenreich, E., & Kundi, M. (1996). Increased inactivation of Saccharomyces cerevisiae by protraction of UV irradiation. *Applied and Environmental Microbiology, 62*(6), 1977–1983. https://doi.org/10.1128/aem.62.6.1977-1983.1996

Unluturk, S., Atilgan, M. R., Baysal, A. H., & Unluturk, M. S. (2010). Modeling inactivation kinetics of liquid egg white exposed to UV-C irradiation. *International Journal of Food Microbiology, 142*(3), 341–347. https://doi.org/10.1016/j.ijfoodmicro.2010.07.013

Vecchio, R., Parga-Dans, E., Alonso González, P., & Annunziata, A. (2021). Why consumers drink natural wine? Consumer perception and information about natural wine. *Agricultural and Food Economics, 9*(1), 1–16. https://doi.org/10.1186/s40100-021-00197-1

Verein Deutscher Ingenieure. (2010). *Vdi heat Atlas*. SpringerLink Bücher. Springer Berlin Heidelberg. https://doi.org/10.1007/978-3-540-77877-6. http://swbplus.bsz-bw.de/bsz329517589cov.htm

Xiang, Q., Fan, L., Zhang, R., Ma, Y., Liu, S., & Bai, Y. (2020). Effect of UVC light-emitting diodes on apple juice: Inactivation of Zygosaccharomyces rouxii and determination of quality. *Food Control, 111*, Article 107082. https://doi.org/10.1016/j.foodcont.2019.107082